J. Plasma Fusion Res. SERIES, Vol. 3 (2000) 352–358

Long Pulse ICRF Heating Experiment on the LHD

KUMAZAWA Ryuhei, MUTOH Takashi, SEKI Tetsuo, WATARI Tetsuo, SAITO Kenji[1)], TORII Yuki[1)], SHIMPO Fujio, NOMURA Goro, YOKOTA Mitsuhiro, HARTMANN Direk.A.[2)], ZHAO Yangping[3)], OKADA Hiroshi[4)], OHKUBO Kunizo, SATO Motoyasu, KUBO Shin, SHIMOZUMA Takashi, IDEI Hiroshi, YOSHIMURA Yasuo, NOTAKE Takashi[1)], TAKITA Yasuyuki, ITOH Satoshi, MIZUNO Yoshiki, KANEKO Osamu, TAKEIRI Yasuhiko, OKA Yoshihide, TSUMORI Katsuyoshi, OSAKABE Masaki, YAMAMOTO Taro[1)], AKIYAMA Ryuichi, KAWAMOTO Toshikazu, ASANO Eiji, OHYABU Nobuyoshi, KAWAHATA Kazuo, KOMORI Akio, YAMADA Hiroshi, AKAISHI Kenya, EMOTO Masahiko, FUNABA Hisamichi, GOTO Motoshi, HAMADA Yasushi, IDA Katsumi, IIZUKA Shinichiro[1)], INAGAKI Shigeru, INOUE Noriyuki, KADO Shinichiro, MASUZAKI Suguru, MINAMI Takashi, MIYAZAWA Jyunichi, MORISAKI Tomohiro, MORITA Shigeru, MURAKAMI Sadayoshi, MUTO Sadatsugu, NAGAYAMA Yoshio, NAKAMURA Yukio, NAKANISHI Hideya, NARIHARA Kazumichi, NISHIMURA Kiyohiko, NODA Nobuaki, KOBUCHI Takashi[5)], OHDACHI Satoshi, OZAKI Tetsu, PETERSON Byron J., SAGARA Akio, SAKAKIBARA Satoru, SAKAMOTO Ryuichi, SASAO Hajime[5)], SASAO Mamiko, SATO Kuninori, SHOJI Mamoru, SUDO Shigeru, SUZUKI Hajime, TANAKA Kenji, TOI Kazuo, TOKUZAWA Toshihiko, YAMADA Ichihiro, YAMAGUCHI Satarou, YAMAZAKI Kozo, YOKOYAMA Masayuki, WATANABE Kiyomasa, MOTOJIMA Osamu, FUJIWARA Masami and LHD Experimental G1 and G2 Group

National Institute for Fusion Science, Toki, 509-5292 Japan

[1)]Nagoya University, Faculty of Engineering, Nagoya, 464-8601 Japan

[2)]Max-Planck-Institute fuer Plasmaphysik, D-85748 Garching, Germany

[3)]Academia Sinica Plasma Physics Institute, Hefei 230031, P.R.China

[4)]Kyoto Univercity, Gokasho, Uji, Kyoto, 611-0011 Japan

[5)]The Graduate University for Advanced Studies, Toki, 509-5292 Japan

(Received: 19 January 2000 / Accepted: 18 April 2000)

Abstract

An Ion Cyclotron Range of Frequency (ICRF) heating experiment on the Large Helical Device has opened up a new field for nuclear fusion research. The plasma was sustained for more than 1 minute by the injected ICRF power only. The injected RF power was 0.8 MW. The plasma stored energy, the line average electron density, the central electron temperature and the ion temperature were 110 kJ, 1.0×10^{19} m^{-3}, 2.0 keV and 2.0 keV, respectively.

Keywords:

ion cyclotron range of frequency heating, long pulse operation, helical system

1. Introduction

The Ion Cyclotron Range of Frequency (ICRF) heating experiment on the Large Helical Device (LHD) [1,2] has been started in the 2nd experimental campaign in 1998 [3,4]. The LHD is a helical device with superconducting coil windings ($l = 2$, $m = 10$), a major radius of 3.9 m and a minor radius of 0.6 m. The main physical

Corresponding author's e-mail: kumazawa@nifs.ac.jp

research is to investigate currentless and disruption-free steady-state plasmas. A maximum plasma stored energy of 0.88 MJ was attained with the heating power of 5 MW in the 3rd experimental campaign [5].

One of the final goals of the ICRF heating on the LHD is the steady-state operation at MW level RF power. Technological research and development have been carried out using a test facility consisting of a transmitter, a dummy load, transmission lines, a co-axial switch, a DC break, an impedance matching circuit, a pre-matching stub tuner, a ceramic feed-through and a test loop antenna installed in a vacuum chamber [6,7]. The transmitter has a capability of wide band frequencies from 25 to 100 MHz. A steady state operation was achieved for 5,000 seconds at an RF power of 1.6 MW [7,8]. Coaxial lines cooled by water have been adopted as components of the transmission lines, whose diameters of outer and inner coaxes are 240 mm and 104 mm, respectively. The steady state test was carried out at the high RF voltage [9]. An innovative liquid stub tuner was tested, and was verified to be usable in the high power operation. In the series of tests, the liquid surface could be shifted during high RF voltage operation, which makes possible the feedback control for the impedance matching in the long pulse ICRF heating [10]. In addition, the vacuum feed-throughs (ceramics Al_2O_3 or Si_3N_4) were tested at 40 kV for 30 minutes [11].

Two different ICRF heating antennas have been fabricated for high power steady state heating and plasma production; one is a loop antenna and the other is a folded wave guide antenna. In the 2nd experimental campaign (1998), a pair of loop antennas was installed on the side of the higher magnetic field strength on the outside of the torus. The folded wave guide antenna was installed in the 3rd experimental campaign (1999).

In the 2nd experimental campaign, ICRF heating experiments were carried out in helium plasma with minority hydrogen ions using a pair of loop antennas at the magnetic field strength B = 1.5 T. The increase in the stored plasma energy was proportional to the applied ICRF heating power up to 300 kW. The maximum increase was found to be 13 kJ at P_{ICH} = 300 kW, which was the same amount as that with ECH only [12].

The 3rd experimental campaign was carried out in 1999. In this paper, the ICRF heating experimental results are described. The injected ICRF heating power was increased to up to 1.5 MW. The frequency f = 38.47 MHz was selected, according to the increased magnetic field strength B = 2.75 T. In Sec.2, the ICRF heating mode using a fast wave is introduced. In Sec. 3, the ICRF heating experimental setup, including a pair of loop antennas and an impedance matching system consisting of three liquid stub tuners, is described. In Sec. 4, the typical ICRF heating experimental results are reported. One is the additional heating to the neutral beam heated plasma and the other is concerned with the long pulse plasma sustained by the ICRF heating. Then we summarize the ICRF heating experiments on the LHD in Sec. 5.

2. ICRF Heating Mode

Fast wave heating has various heating scenarios, which are referred to as minority, mode conversion and 2nd harmonic heating methods. One of these can be selected by choosing the magnetic field strength, the frequency and the ion species. The ICRF heating efficiency depends mainly on the location of the minority ion cyclotron resonance and the ion-ion hybrid resonance layers. Figure 1 shows a typical heating scenario referred to as Mode-I, in which the ICRF heating experiments in the 3rd campaign were mainly carried out. The minority cyclotron resonance, L (left hand) cutoff, R (right hand) cutoff and ion-ion hybrid resonance (in dotted line) layers are plotted in Fig.1. Here the magnetic field strength, the frequency and the

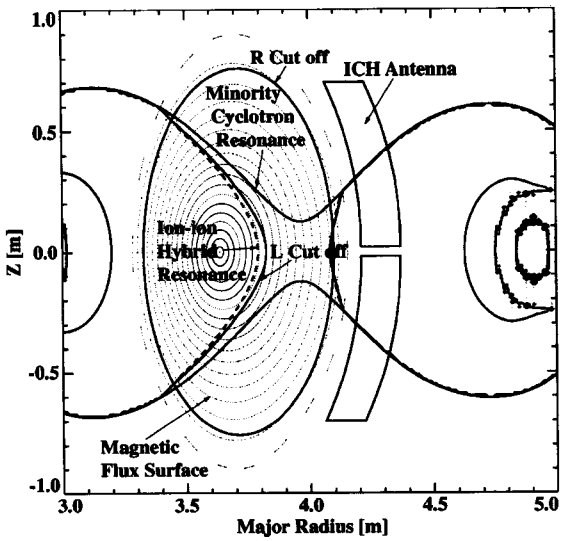

Fig. 1 ICRF heating mode referred to as Mode-I: Locations of ion cyclotron resonance of minority ions, ion-ion hybrid resonance, R cutoff and L cutoff are plotted in the case of the electron density of $n_e(0) = 1.0 \times 10^{19}\,m^{-3}$, n_H/n_e = 10%, B = 2.75T and f = 38.47 MHz.

wave number are B = 2.75 T, $f = \omega/2\pi$ = 38.47 MHz and $k_{//} = 5\ m^{-1}$, respectively. The plasma parameters are the central electron density, $n_e(0) = 1.0 \times 10^{19}\ m^{-3}$ and the minority hydrogen ratio of 10% in the helium plasma. The ion-ion hybrid resonance is located between the magnetic axis and the minority ion cyclotron resonance, which is located at the lower magnetic field side, the same as in CHS experiment [13]. As the ratio of the hydrogen ions to the helium ions becomes higher, the hybrid resonance layer moves toward the magnetic axis. When the frequency is decreased or the magnetic field strength is increased, the ion cyclotron resonance layer moves toward the lower magnetic field. According to the shift of the cyclotron resonance layer, the ion-ion hybrid resonance layer also moves to the lower magnetic field side and is separated into two layers; that is referred to as Mode-II. The fast wave launched from the ICH antenna accesses from the higher magnetic field side. The dominant electron heating is expected via a mode conversion to ion Bernstein wave rather than the ion heating.

The installed antennas, which will be described in detail in the next section, are also shown in this figure. The distance between the top of the side limiter and the last closed magnetic surface was usually selected at 5 cm in the series of experiments.

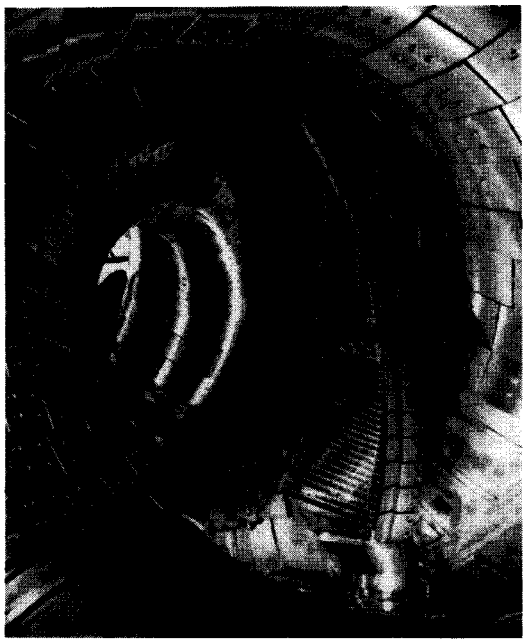

Fig. 2 A pair of ICRF heating antennas is installed at the higher magnetic field side on the outside of the torus in the LHD.

3. Experimental Setup

The ICRF heating experiments were carried out using a pair of loop antennas. The loop antennas are installed from an upper and a lower vertical vacuum port as shown in Fig. 2. The antennas are located on the higher magnetic field side on the outside of the torus. The antenna is 60 cm in length, 46 cm in width and 17 cm in depth. The antenna strap is 30 cm in width. The surface of the antenna is fitted to a configuration of the last closed magnetic surface. The position of the ICH antenna can be shifted inward by 15 cm by using a swing mechanism. The direction of Faraday shield with a single layer is parallel to the magnetic line of force at the last closed magnetic flux surface.

The RF power is transmitted to each antenna from the high power RF generator via a liquid impedance matching system. It consists of three liquid stub tuners, which are identical. The length of the liquid stub tuners is 4.5 m. The triple liquid impedance matching system has the merit of having a wider tunable frequency range than that in a double stub tuner system.

The characteristic impedance of the co-axial transmission line is 50 Ω. All the RF components of the transmission lines, including the liquid stub tuners and the loop antennas, are cooled by purified water to achieve a high RF power steady state operation.

The ratio of the minority to the majority ions is a key parameter for optimizing minority or mode conversion heating. In the ICRF heating experiment, hydrogen ions are used as a minority in the helium plasma. An optical measurement method is employed to estimate the ratio of the hydrogen minority ions. The spectroscopic apparatuses are installed at the vacuum port adjacent to the ICH antenna to monitor Hα (656.3 nm) and HeI (587.6 nm) signals.

Hydrogen or helium glow discharge cleaning was carried out for the wall conditioning with titanium gettering, which covered about 30% of the LHD vacuum vessel surface. The vacuum base pressure was maintained in the middle of 10^{-7} Pa.

4. Experimental Results

4.1 Plasma loading resistance

The RF power generated by an RF power source is transmitted via the triple liquid impedance matching system to the ICH antennas, i.e. the U-antenna and the L-antenna. A phase difference between the two antennas is one of the parameters controlled to maximize the ICRF heating power. The opposite phase was adopted in

the series of the ICRF heating experiments, in which the fast wave is launched in a low poloidal mode number. When the phase is not just opposite, the plasma loading resistance becomes unbalanced between in the U and L antennas, but the summation is almost constant.

The plasma loading resistance depends on both the electron density and the distance between the antenna and the last closed magnetic flux surface. The plasma loading resistance is from 3 Ω to 5 Ω in the range of the line average electron density, 1×10^{19} m^{-3} < $\bar{n}_e$ < 4×10^{19} m^{-3}. As the vacuum loading is measured to be 0.75 Ω, the injection efficiency is calculated to range from 75% to 85%, which is defined as the fraction of the radiated power from the ICH antenna to the transmitted power from the RF power generator. The plasma loading resistance also depends on the antenna position. The plasma loading resistance gradually decreases with the antenna distance from the last closed magnetic surface. However the loading resistance at 9.5 cm was still 77% of that at 5 cm.

4.2 Additional ICRF heating to NNBI heated plasma

The ICRF heating quality was examined on the negative-based neutral beam injection (NNBI) plasma at a different electron density, 1×10^{19} m^{-3} < $\bar{n}_e$ < 3.3×10^{19} m^{-3}. The counter injection of NNBI was used and the port-through power of NNBI was almost constant at P_{pt} = 1.45 MW (E_{inj} = 130 keV) in the series of experiments. The time evolutions of various plasma parameters are plotted in Fig. 3. The plasma stored energy, W_p, the line average electron density, $\bar{n}_e$, the electron temperature on axis, T_{e0} and the radiated power, P_{rad} are plotted with an intensity ratio of Hα to HeI for the case of the line average electron density, $\bar{n}_e = 2.0 \times 10^{19}$ m^{-3} as shown in Fig. 3. The plasma stored energy was increased from 230 kJ to 340 kJ with P_{ICH} = 1.2 MW, which is the radiated RF power from the antennas.

In this shot, the absorbed power of NNBI is P_{NBI} = 1.2 MW, which is calculated by measurement of the temperature increase of the armor tiles [14].

On the other hand, the RF power absorbed by the plasma can be estimated by the decay of the plasma stored energy. The heating efficiency was 81%. Experiments were carried out for the three different cases of the line average electron density, i.e. 1.0×10^{19} m^{-3}, 2.0×10^{19} m^{-3} and 3.3×10^{19} m^{-3} as shown in Fig. 4. These experimental data can be compared with the calculated plasma store energy by solid lines using a power dependence of International Stellarator Scaling

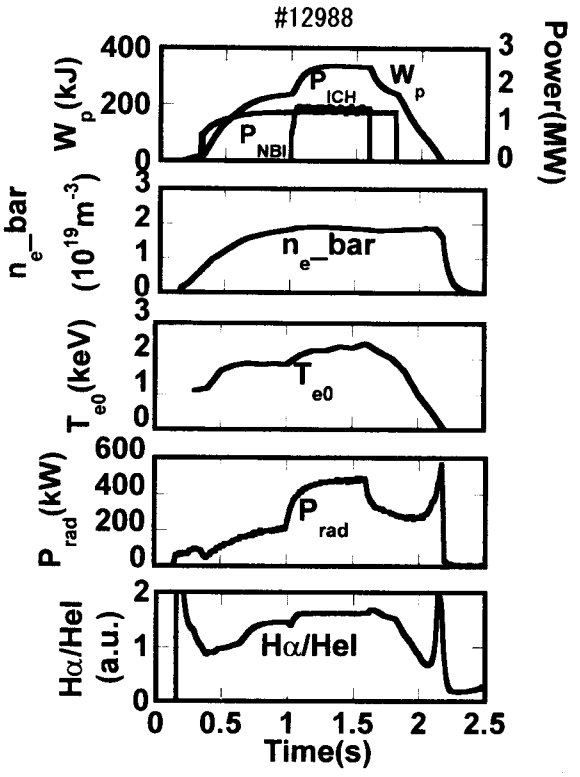

Fig. 3 Time evolutions of plasma parameters of the additional ICRF heating to the neutral beam heated plasma at the line average electron density of $\bar{n}_e = 2.0 \times 10^{19}$ m^{-3}.

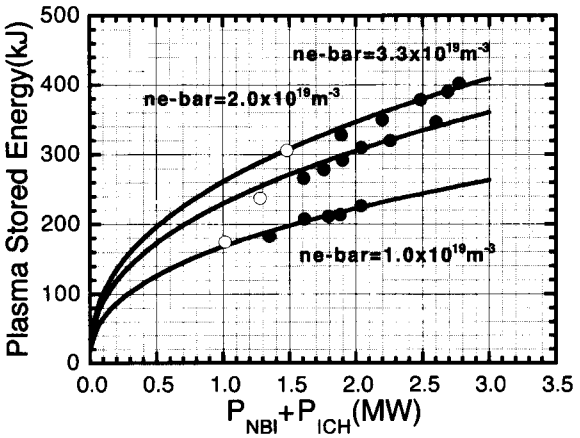

Fig. 4 The dependence of the plasma stored energy on the total heating power, P_{NBI} + P_{ICH} for the three different electron densities. Open and solid circles indicate the plasma stored energy with only NNBI heating and with the additional ICRF heating, respectively.

(ISS95). It is found that the ICRF heating is comparable with the NNBI heating.

4.3 ICH sustained plasma

The plasma was sustained by injecting ICRF heating power only. An initial plasma was started by fundamental Electron Cyclotron Heating (ECH, 82.6 and 84.0 GHz with 0.4–0.5 MW). The ICRF heating power was applied to the ECH plasma 0.1–0.2 second before the turn-off of the ECH. After the ECH turn-off the plasma could be sustained by an ICRF heating larger than 0.5 MW. The ICRF heating quality of the sustained plasma was examined by changing the magnetic field strength from B = 2.5 T to 2.9 T at the fixed applied frequency f = 38.47 MHz. The observed plasma stored energy was maximized at B = 2.75 T. The ratio of the hydrogen to helium ions, Hα/HeI is also a key for optimizing the ICRF heating as described in the previous section. The optimal ratio is around one; the ratio of the minority hydrogen ion to the electron density was deduced to be about 10%.

A typical discharge of the ICH sustained plasma with P_{ICH} = 1.3 MW is shown in Fig. 5. The average line electron density is $\bar{n}_e = 1.8 \times 10^{19}$ m^{-3} with the stored plasma energy of 200 kJ. In this operation, the intensity ratio of Hα to HeI was maintained between 0.8 and 0.7. The electron density was adjusted by using a helium gas puffing. The hydrogen ion density was maintained by the recycling from the vacuum wall. The electron temperature is 1.7 keV at the magnetic axis. The radiated power was observed to be P_{rad} = 300–400 kW during the ICRF heating. The parameters of the ICH-sustained plasma are similar to those of the NNBI plasma with the same absorbed power level.

A neutral diamond detector detected ions heated by RF electric field in the energy range from 20 keV to 200 keV [15]. The effective ion temperature, which depended on the electron temperature and density of the bulk plasma was measured to be from 10 keV to 50 keV. It can be interpreted using the Stix formula [16].

The RF power absorbed by electrons was derived from the decay rate of the electron cyclotron emission measurement after the turn-off of the ICRF heating power. Then the fraction of the electron absorption power was found to be small. Therefore, minority ions were considered to absorb almost all the injected ICRF heating power.

The energy confinement times of ICH-sustained (open circles), NNBI-sustained (open squares) and ICH + NNBI (open triangles) plasmas were compared with

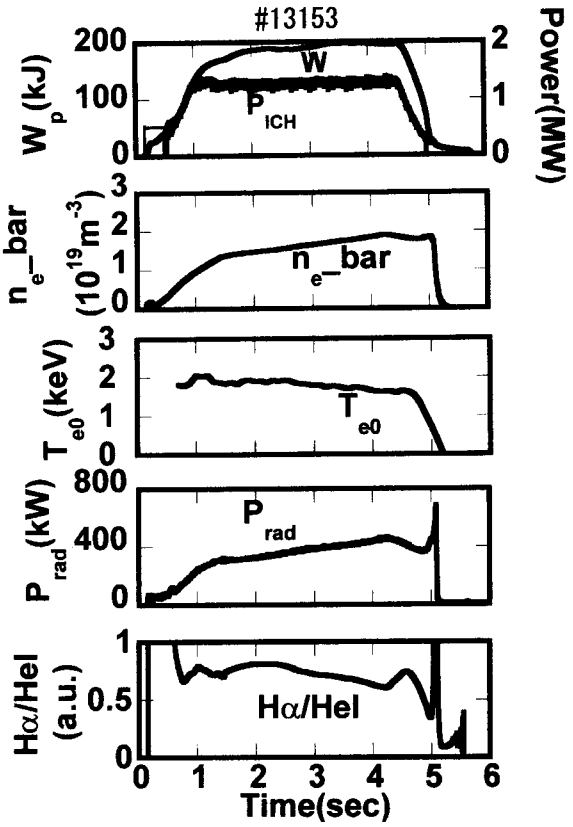

Fig. 5 Time evolutions of parameters of the plasma sustained by ICRF heating at the average line electron density of $\bar{n}_e = 1.8 \times 10^{19}$ m^{-3} with P_{ICH} = 1.3 MW.

ISS95 as shown in Fig. 6. The absorbed power, deduced from the decay of the plasma stored energy was used here. The improvement factor is found to be over 1.5. It was founded to be larger at the lower energy confinement, which was obtained at the relatively low electron density.

4.4 Long pulse of ICH sustained plasma

A long pulse operation was tried at the end of the 3rd experimental campaign, using ICRF heating. The pulse length was lengthened shot by shot from 5 to 45 seconds in order to age the tetrode tubes of the final amplifier. The pulse duration time of ICH-sustained plasma could be prolonged up to 68 seconds as shown in Fig. 7. The radiated RF power from the antennas, the average plasma stored energy, the average electron density, the electron temperature on the magnetic axis, the ion temperature and the radiation power are P_{ICH} = 0.8 MW, W_p = 110 kJ, $\bar{n}_e = 1.0 \times 1019$ m^{-3}, T_{e0} = 2.0 keV, T_i = 2.0 keV and P_{rad} = 200 kW, respectively. The

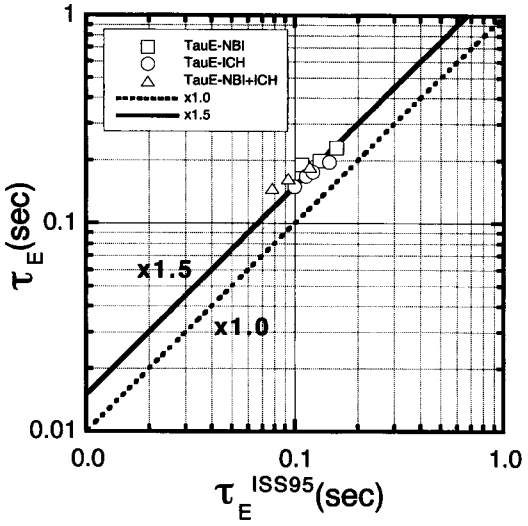

Fig. 6 Energy confinement times of the ICH and NNBI heated plasmas are compared with those calculated using ISS95. Open circles, squares and triangles indicate ICRF heating, the NNBI heating and the simultaneous heating of NNBI and ICRF heating, respectively. Solid and dotted lines show the improvement factor.

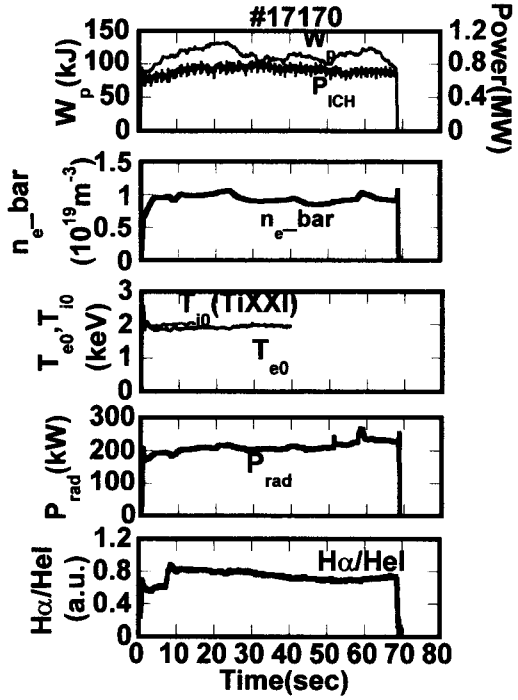

Fig. 7 Time evolutions of parameters of the long pulse plasma sustained by ICRF heating at the average line electron density of $\bar{n}_e = 1.0 \times 10^{19}$ m^{-3} with P_{ICH} = 0.8 MW.

ion temperature was measured from Doppler broadening of TiXXI (0.261 nm) using an X-ray crystal spectrometer [17]. During this operation, the minority fraction was kept constant at Hα/HeI = 0.7 as also shown in Fig. 7. After this shot, hot spots on the side carbon limiter were observed. However serious damage could not be found there by inspecting after opening the LHD to the air. The duration time was limited by the shutoff of the RF power generator due to the interlock of the over current at the tetrode grid current. A more extended long pulse operation, e.g. 30 minutes, will be able to be achieved by adopting the optimal operation such as a low impedance mode [6-8]. The reflected power fraction gradually increased but was less than 10%. When the longer operation is attempted in the next trial, the feedback control impedance matching using the liquid stub tuner will be required [10].

5. Summary

ICRF heating experiments on the LHD have demonstrated excellent results with regard to the additional heating to the NNBI plasma and the ICH-sustained plasma with high stored energy up to 200 kJ and with a long pulse operation up to 68 seconds at 1 MW level of RF power. The confinement characteristic of the ICRF heating is the same as that of the NNBI. Another two pairs of identical antennas will be installed to triple the ICRF heating power in the coming experimental campaign.

Acknowledgements

The authors would like to thank the scientists and the technical staff at the National Institute for Fusion Science who made these experiments possible and especially the former director-general, Professor A. Iiyoshi.

References

[1] A. Iiyoshi and K.Yamazaki, Phys of Plasmas, **2(6)**, 2349 (1995).
[2] O. Motojima, K. Akaishi *et al.*, Fusion Eng. Des., **20**, 3 (1993).
[3] A. Iiyoshi *et al.*, IAEA-F1-CN-69, OV1/4 (1998).
[4] M. Fujiwara *et al.*, IAEA-F1-CN-69/EX2/3 (1998).
[5] O. Motojima *et al.*, this conference. I-1.
[6] T. Watari *et al.*, IAEA-F1-CN-69/FTP/21 (1998).
[7] T. Seki, R. Kumazawa *et al.*, this conference, PII-2.
[8] R. Kumazawa *et al.*, Proceeding of 18th Symposium on Fusion Technology Vol.1, 617 (1996).
[9] R. Kumazawa *et al.*, Journal of Plasma and Fusion

Research, Vol.**75**, 842 (1999).
[10] R. Kumazawa *et al.*, Rev. Sci. Instrum., **70**, 555 (1999).
[11] T. Mutoh *et al.*, Fusion Eng. Des., **26**, 387 (1999).
[12] R. Kumazawa *et al.*, 13th Topical Conference on Radio Frequency Power in Plasmas, **485**, 160 (1999).
[13] S. Masuda, R.Kumazawa *et al.*, Nucl. Fusion, Vol.**37**, 53 (1997).
[14] M. Osakabe *et al.*, to be submitted to Review of Scientific Instruments.
[15] A. Klashilnikov, M. Isobe, M. Sasao. *et al.*, to be submitted to Review of Scientific Instruments.
[16] T.H. Stix, Nucl Fusion **15**, 737 (1975).
[17] S. Morita *et al.*, Proc. 14th European Conference on Controlled Fusion and Plasma Physics, Vol.IID, Part III 874 (1987).